

Linear feedback control of transient energy growth and control performance limitations in subcritical plane Poiseuille flow

F. Martinelli* and M. Quadrio

*Politecnico di Milano, Dipartimento di Ingegneria Aerospaziale,
Via La Masa 34, Milano, Italy*

J. McKernan

*Experimental & Computational Laboratory for the Analysis of Turbulence,
King's College London,
Strand, London WC2R 2LS, U.K.*

J.F. Whidborne

*Department of Aerospace Sciences, Cranfield University,
Cranfield, Bedfordshire, MK43 0AL, U.K.*

Suppression of the transient energy growth in subcritical plane Poiseuille flow via feedback control is addressed. It is assumed that the time derivative of any of the velocity components can be imposed at the walls as control input, and that full-state information is available. We show that it is impossible to design a linear state-feedback controller that leads to a closed-loop flow system without transient energy growth. In a subsequent step, full-state feedback controllers – directly targeting the transient growth mechanism – are designed, using a procedure based on a Linear Matrix Inequalities approach. The performance of such controllers is analyzed first in the linear case, where comparison to previously proposed linear-quadratic optimal controllers is made; further, transition thresholds are evaluated via Direct Numerical Simulations of the controlled three-dimensional Poiseuille flow against different initial conditions of physical interest, employing different velocity components as wall actuation. The present controllers are effective in increasing the transition thresholds in closed loop, with varying degree of performance depending on the initial condition and the actuation component employed.

I. INTRODUCTION

Transient energy growth has been recognized as a possible mechanism explaining subcritical transition in wall-bounded flows; in fact, subcritical flows may experience large transient amplifications of the energy of perturbations, that could trigger nonlinear mechanisms and eventually lead to transition to turbulence^{1–3}.

In viscous shear flows, transient energy growth is related to the non-normality of the linearized Navier-Stokes operator with respect to the energy inner product^{4,5}. In the last few years, several investigators attempted to reduce the transient growth phenomenon in Poiseuille and boundary layer flows by employing wall actuation and applying linear control theory to an appropriate discretization of the linearized equations. In their seminal work on feedback control of instabilities in two-dimensional Poiseuille flow, Joshi et al.⁶ employed a compensator in the form of a constant-gain integral feedback, and demonstrated stabilization of the linearly unstable flow as well as attenuation of finite amplitude disturbances. They further pointed out that transient amplifications in the flow energy may not be properly detected by the sen-

sors, and also that the control itself may trigger non-linear mechanisms by introducing transient disturbances on short times. Leveraging a state-space formulation obtained after discretization of the boundary-controlled Orr-Sommerfeld-Squire equations, optimal and robust control theory was applied to transitional channel flows by Bewley & Liu⁷ for a single wavenumber pair and by Högberg et al.⁸ for a large array of wavenumber pairs, leading to a reduction of the maximum transient energy growth as well as an increase in transition thresholds. It has been recently shown⁹ that the linear coupling term in the Orr-Sommerfeld-Squire equations plays a role not only in the non-normal behavior of the small perturbation dynamics, but also in the self-sustaining process of near-wall, low Reynolds number turbulence. This evidence led investigators to test in turbulent channel flows the optimal controllers designed on linearized flow models, and encouraging results have been obtained in terms of drag reduction^{10–13}. Feedback control of non-modal disturbances in boundary layer flows has been recently considered by Corbett & Bottaro¹⁴ in the framework of optimal control theory, while Zuccher et al.¹⁵ applied steady suction in the attenuation of the growth of given optimal disturbances in a Blasius boundary layer.

Although it has been demonstrated¹³ that optimal and robust control laws are well suited for reducing the non-normal behavior of fluid flow systems, to date no feedback control law has been devised with the capability of

*Present address: LadHyX, École Polytechnique, F-91128 Palaiseau, France. e-mail: fulvio.martinelli@polimi.it

ensuring closed-loop monotonic stability, when boundary actuation is employed. It is therefore natural to ask whether such performance can be obtained with a linear feedback, and further which control techniques are available to directly target the transient growth mechanism. In the controls literature, the transient amplification of certain norms of the state bears the name of *peaking phenomenon* and the monotonic stability requirement is generally referred to as *strict dissipativity*. Active controllers with the capability of targeting transient norm amplifications have received attention in the analysis of a class of partially linear cascade systems¹⁶, and more recently in conjunction with a Linear Matrix Inequality (LMI) approach^{17,18}. In a very recent paper, Whidborne & McKernan¹⁹ extended these results giving conditions on the existence of a feedback controller ensuring the strict dissipativity of the closed-loop system. These results were then exploited by Whidborne et. al²⁰, who considered the feedback control of a single wavenumber pair in plane Poiseuille flow via LMI design and wall-normal blowing and suction, and by Martinelli et al.²¹, where LMI-based feedback controllers have been designed and tested for an array of wavenumber pairs. The present paper aims at expanding and completing these recent results, by showing first that it is impossible to design a linear state-feedback controller ensuring the plane Poiseuille flow – controlled via wall transpiration with any velocity component – to be strictly dissipative. In a second step, feedback control laws are designed using an LMI technique, for an array of wavenumber pairs; their performance is compared against that of optimal controllers in the linear case, and furthermore closed-loop transition thresholds are evaluated for optimal initial conditions in the form of a pair of oblique waves and antisymmetric streamwise vortices, at the Reynolds number $Re = 2000$, using different velocity components as wall actuators.

II. MODEL OF THE SYSTEM

We consider the dynamics of three-dimensional small perturbations to the laminar Poiseuille solution in a plane channel. A Cartesian coordinate system is introduced, where x , y and z denote the streamwise, wall-normal and spanwise directions, and u , v , w denote the corresponding perturbation velocity components. The Navier-Stokes equations, linearized about the laminar solution $U(y) = U_p(1 - (y/\delta)^2)$, are non-dimensionalized with the centerline velocity U_p and the channel half-width δ , and rewritten in the form of a single equation for v one-way coupled to an equation for the wall-normal vorticity $\eta = \partial u/\partial z - \partial w/\partial x$. Fourier transformation in x and z direction yields the well known Orr-Sommerfeld-Squire form:

$$\begin{aligned}\Delta \dot{\tilde{v}} &= [-j\alpha U \Delta + j\alpha U'' + \Delta \Delta / Re] \tilde{v} \\ \dot{\tilde{\eta}} &= [-j\beta U'] \tilde{v} + [-j\alpha U + \Delta / Re] \tilde{\eta}\end{aligned}\quad (1)$$

at the wavenumber pair (α, β) . Here, the tilde denotes Fourier coefficients, the dot denotes time derivative, the prime denotes y differentiation, $\kappa^2 = \alpha^2 + \beta^2$, j is $\sqrt{-1}$, and $\Delta = d^2/dy^2 - \kappa^2$.

We select boundary conditions representing time-varying wall transpiration on any of the velocity components at the two channel walls (“vectorized transpiration”). In turn, this results in inhomogeneous Dirichlet and Neumann conditions on \tilde{v} , as well as inhomogeneous Dirichlet conditions on $\tilde{\eta}$:

$$\begin{aligned}\tilde{v}(y = \pm 1, t) &= \tilde{v}_{u,l}(t), \\ \partial \tilde{v} / \partial y (y = \pm 1, t) &= \tilde{v}'_{u,l}(t), \\ \tilde{\eta}(y = \pm 1, t) &= \tilde{\eta}_{u,l}(t).\end{aligned}\quad (2)$$

A standard lifting procedure⁸ is then employed, i.e. the unknowns are rewritten as homogeneous components (satisfying homogeneous boundary conditions) plus inhomogeneous components thus:

$$\begin{aligned}\tilde{v}(y, t) &= \tilde{v}_h(y, t) + f_u(y)\tilde{v}_u(t) + f_l(y)\tilde{v}_l(t) + \dots \\ &\dots + g_u(y)\tilde{v}'_u(t) + g_l(y)\tilde{v}'_l(t) \\ \tilde{\eta}(y, t) &= \tilde{\eta}_h(y, t) + h_u(y)\tilde{\eta}_u(t) + h_l(y)\tilde{\eta}_l(t),\end{aligned}\quad (3)$$

where $f_u, f_l, g_u, g_l, h_u, h_l$ are polynomials in y chosen to satisfy unitary boundary conditions for each lifted component appropriately.

We discretise the homogeneous components \tilde{v}_h and $\tilde{\eta}_h$ in wall-normal direction using a modified Chebyshev series cardinal function basis

$$\begin{aligned}\tilde{v}_h(y, t) &= \sum_{n=0}^{N-4} \Gamma_n^{DN}(y) a_{v,n}(t) \\ \tilde{\eta}_h(y, t) &= \sum_{n=0}^{N-2} \Gamma_n^D(y) a_{\eta,n}(t)\end{aligned}\quad (4)$$

where the modified Chebyshev functions $\Gamma_n^{DN}(y)$ and $\Gamma_n^D(y)$ implicitly enforce the required homogeneous Dirichlet and Neumann boundary conditions, lead to good conditioning of the discrete Laplacian operator, and no spurious modes are generated²². The Orr-Sommerfeld-Squire equations are then evaluated on a set of Gauss-Lobatto collocation points in y direction and rearranged to have the time rate of change of actuation velocity as an input⁸. This results in the the linear time-invariant system model²³

$$\dot{\tilde{\mathbf{x}}}(t) = \overline{\mathbf{A}}\tilde{\mathbf{x}}(t) + \overline{\mathbf{B}}\mathbf{u}(t), \quad \tilde{\mathbf{x}}(0) = \tilde{\mathbf{x}}_0,$$

where $\overline{\mathbf{A}}$, $\overline{\mathbf{B}}$ are constant system and input matrices, and \mathbf{u} , $\tilde{\mathbf{x}}$ are respective input and state vectors. As noted in previous work⁸, the natural outcome of this procedure is an augmented state-space form, where additional integrators associated to the values of the input velocity components at the walls are explicitly introduced. Consequently, the *open-loop* dynamics of the system above (i.e. setting $\overline{\mathbf{B}} = 0$) is different from the dynamics of the

original, *unactuated* system (where the velocity at the walls is fixed by the no-slip condition). This terminology will be used throughout the paper to distinguish between the two cases.

The kinetic energy per unit mass of flow perturbations in the volume V

$$E = \frac{1}{2V} \int_V u^2 + v^2 + w^2 dV$$

can be expressed as a function of the state vector $\bar{\mathbf{x}}$ using the continuity equation, the definition of η , and Parseval's identity:

$$E = \sum_{(\alpha, \beta)} \tilde{E}(\alpha, \beta) = \sum_{(\alpha, \beta)} \bar{\mathbf{x}}^H \mathbf{Q}(\alpha, \beta) \bar{\mathbf{x}}$$

where the matrix \mathbf{Q} is an Hermitian, positive definite matrix; here, the superscript H denotes conjugate transpose. In the following, we have transformed the state vector via the change of variable $\mathbf{x} = \mathbf{C}\bar{\mathbf{x}}$ (\mathbf{C} being the Cholesky factor of \mathbf{Q}) in order to rewrite the system dynamics as

$$\dot{\mathbf{x}}(t) = \mathbf{A}\mathbf{x}(t) + \mathbf{B}\mathbf{u}(t), \quad \mathbf{x}(0) = \mathbf{x}_0, \quad (5)$$

such that the system energy is directly given by the Euclidean norm $\mathbf{x}^H \mathbf{x}^{5,23}$.

III. CLOSED-LOOP MONOTONIC STABILITY

We consider the linear time-invariant system model (5) and further assume that $\mathbf{B}^H \mathbf{B} > 0$, that is \mathbf{B} has full column rank (i.e. all the actuators are independent – a condition which is trivially satisfied in the present problem). Contraction analysis for this kind of system has been presented by Whidborne & McKernan¹⁹ and, in the general case of nonlinear systems, by Lohmiller & Slotine²⁴. In particular, referring to the linear case, it has been shown¹⁹ that there exists a static state-feedback controller $\mathbf{u} = \mathbf{K}\mathbf{x}$, where \mathbf{K} is a constant matrix, such that the closed-loop system has strict dissipativity (i.e. energy $\mathbf{x}^H \mathbf{x}$ decays monotonically from all initial conditions \mathbf{x}_0), if and only if

$$\mathbf{B}^\perp (\mathbf{A} + \mathbf{A}^H) \mathbf{B}^{\perp H} < 0 \text{ or } \mathbf{B}\mathbf{B}^H > 0, \quad (6)$$

where \mathbf{B}^\perp is the left null space of \mathbf{B} . Additionally¹⁹ if no static controller that achieves strict dissipativity exists, then no dynamic state-feedback controller, where \mathbf{u} is given from \mathbf{x} by the dynamic system

$$\dot{\mathbf{x}}_k(t) = \mathbf{A}_k \mathbf{x}_k(t) + \mathbf{B}_k \mathbf{x}(t), \quad \mathbf{x}_k(0) = \mathbf{x}_{k0}, \quad (7)$$

$$\mathbf{u}(t) = \mathbf{C}_k \mathbf{x}_k(t) + \mathbf{D}_k \mathbf{x}(t), \quad (8)$$

where $\mathbf{A}_k, \mathbf{B}_k, \mathbf{C}_k$ and \mathbf{D}_k are constant matrices and \mathbf{x}_k are controller states, exists either.

It is immediate to verify that the second criterion in (6) is never satisfied in the present system, as the Hermitian

matrix $\mathbf{B}\mathbf{B}^H$ is never positive definite but it is always positive semidefinite, because the dimension of the input vector is always smaller than that of the state vector. In order to have $\mathbf{B}\mathbf{B}^H > 0$, a number of independent actuators equal to the number of flow states is required; this is a situation that is unlikely to occur in practical flow control problems, where normally actuators are placed at the walls. Even when volume forcing is available, this condition is unlikely to be satisfied, since practical volume forces are not as flexible as to enforce an arbitrary force distribution in the entire flow domain at any time instant.

The first algebraic criterion in Eq. (6) is equivalent to requiring that the portion of the system dynamics which is not accessible by the controls must be dissipative. Verifying this criterion is not trivial. Here we evaluate it numerically, in order to identify those regions in the (α, β, Re) parametric space where subcritical Poiseuille flow may be rendered monotonically stable by feedback transpiration. To this aim, the state-space model (5) is first obtained on a fine grid and, as suggested by Reddy & Henningson², a limited number N_t of eigenfunctions is retained, discarding those corresponding to highly damped and poorly resolved eigenvalues. Properly rescaling the variables such that energy is written as an Euclidean norm leads to a reduced order model $\mathbf{A}_r, \mathbf{B}_r$, and the negative-definiteness of the corresponding matrix $\mathbf{B}_r^\perp (\mathbf{A}_r + \mathbf{A}_r^H) \mathbf{B}_r^{\perp H}$ in (6) is verified by computing its maximum (real) eigenvalue λ_{max} . Figure 1 shows the present result on the (Re, α) plane for $\beta = 0$, along with the well-known result on the transient growth dependence in plane Poiseuille flow² (i.e. the unactuated case). The white area corresponds to the domain where the unactuated system is monotonically stable, while the shaded area is the region where the unactuated system admits transient energy growth. Solid lines correspond to isocontours of λ_{max} , and it appears that the contour $\lambda_{max} = 0$ lies on the very boundary between the shaded and white area, implying that the Hermitian matrix $\mathbf{B}_r^\perp (\mathbf{A}_r + \mathbf{A}_r^H) \mathbf{B}_r^{\perp H}$ is indefinite when the unactuated system is not monotonically stable. An analogous result is reported in Fig. 2, where isocontours of λ_{max} are reported on the plane (α, β) , at $Re = 120$; again, the contour $\lambda_{max} = 0$ lies on the boundary between the regions of monotonic and non-monotonic stability. From the aforestated theorem¹⁹, this implies that it is not possible to design a state-feedback controller that ensures the closed loop Poiseuille flow to be monotonically stable, when the corresponding unactuated flow is not.

This result shows an inherent limitation in the feedback control of the transient growth mechanism, when vectorized wall transpiration in terms of time rate of change of zero net-mass flux blowing/suction is employed. Note that vectorized transpiration, although being rather idealized, exploits all the degrees of freedom available for boundary control in the present problem; therefore, the present result is representative of a limiting

situation. In a practical setting, actuator-dependent constraints may introduce additional mechanisms restricting the control authority even more. It is also worth mentioning that strict dissipativity is a rather tough requirement for a controller bound to operate on a largely underactuated flow, and in fact an approach based on strict dissipativity is in general quite conservative, i.e. some energy growth is tolerable in transition control. Finally, it should be emphasized that the present analysis is limited to linear feedback laws, and that performance of nonlinear controllers may be more promising. For example, it has been shown²⁵ that introducing a nonlinearity in the form of gain-scheduling on full-state feedback laws led to relaminarization of low- Re turbulence even employing wall actuation only, and that adjoint-based optimization on the nonlinear turbulent flow can be successfully employed in feedback relaminarization¹¹.

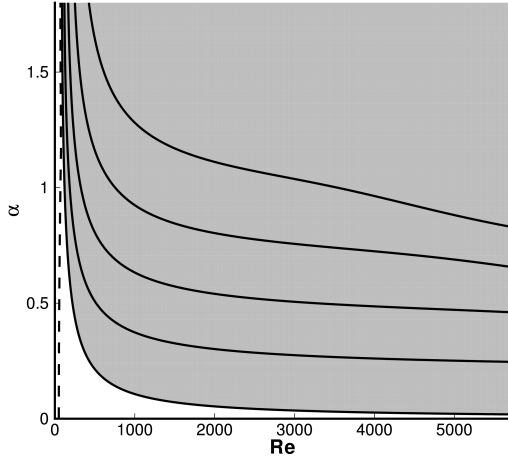


FIG. 1: Numerical verification of the first algebraic criterion in Eq. (6). Lines: contours at constant $\lambda_{max}(Re, \alpha)$, at $\beta = 0$. Levels are from -0.1 to 0.4 by 0.1 increments; dashed line is negative value. The shaded area corresponds to the region where the unactuated system is not monotonically stable, i.e. admits transient energy growth. The contour $\lambda_{max}(Re, \alpha) = 0$ lies on the boundary of the region, indicating that no state-feedback controller can be designed to ensure strict dissipativity of the closed-loop system when the unactuated system is not strictly dissipative. Results obtained with $N = 100$, $N_t = 50$.

IV. UPPER-BOUND MINIMIZING FEEDBACK CONTROLLER

In order to design a state-feedback controller with the capability of targeting the transient growth mechanism directly, an estimate of the maximum transient growth is required. Such estimate is obtained as an upper bound on the maximum growth via Lyapunov theory. For the

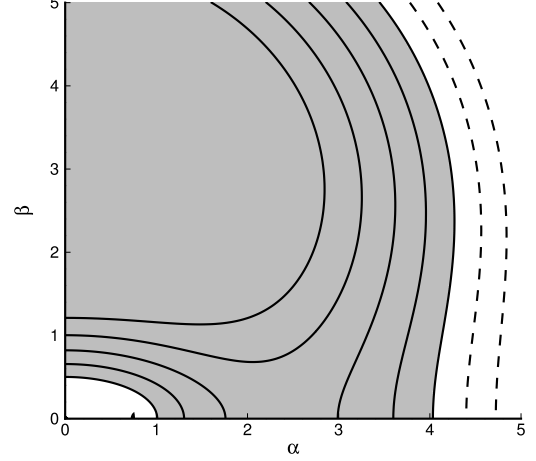


FIG. 2: Numerical verification of the first algebraic criterion in Eq. (6). Results for $Re = 120$, levels are from -0.1 to 0.2 by 0.05 increments. For details see caption of Fig. 1.

linear, time invariant, asymptotically stable system:

$$\dot{\mathbf{x}} = \mathbf{A}\mathbf{x}, \quad \mathbf{x}(0) = \mathbf{x}_0,$$

it can be shown that an upper bound on the maximum transient growth G is given by^{19,20} :

$$G_u = \lambda_{max}(\mathbf{P})\lambda_{max}(\mathbf{P}^{-1}) \geq G,$$

where $\mathbf{P} = \mathbf{P}^H > 0$ satisfies the Lyapunov inequality

$$\mathbf{P}\mathbf{A} + \mathbf{A}^H\mathbf{P} < 0.$$

A minimal upper bound can be obtained by solving the following minimization problem²⁶ :

$$\begin{aligned} \min \gamma : \\ \mathbf{P}\mathbf{A} + \mathbf{A}^H\mathbf{P} < 0, \quad \mathbf{P} = \mathbf{P}^H > 0 \\ \mathbf{I} < \mathbf{P} < \gamma\mathbf{I}, \end{aligned} \quad (9)$$

where the last inequality ensures $\gamma > G_u$. The problem stated in Eq. (9) is a LMI generalized eigenvalue problem, and standard solution methods based on interior point algorithms are available²⁷.

An analogous problem to that stated in Eq. (9) can be obtained if the feedback minimization of the upper bound is of interest. Indeed, let us consider the system (5) along with a state-feedback control law in the form $\mathbf{u} = \mathbf{K}\mathbf{x}$, so that in closed-loop the system dynamics is described by:

$$\dot{\mathbf{x}} = (\mathbf{A} + \mathbf{B}\mathbf{K})\mathbf{x}, \quad \mathbf{x}(0) = \mathbf{x}_0.$$

Leveraging the additional degrees of freedom due to the controller gains \mathbf{K} , we move to minimizing the closed-loop upper bound on the maximum transient growth. The associated Lyapunov inequality now reads:

$$\mathbf{P}\mathbf{A} + \mathbf{A}^H\mathbf{P} + \mathbf{P}\mathbf{B}\mathbf{K} + \mathbf{K}^H\mathbf{B}^H\mathbf{P} < 0;$$

this inequality can be rewritten in the LMI form by recalling that a similarity transformation preserves the eigenvalues. Therefore, defining $\mathbf{Q} = \mathbf{P}^{-1}$ and $\mathbf{Y} = \mathbf{K}\mathbf{Q}$, the closed-loop upper-bound minimization problem can be written as²⁶

$\min \gamma :$

$$\mathbf{A}\mathbf{Q} + \mathbf{Q}\mathbf{A}^H + \mathbf{B}\mathbf{Y} + \mathbf{Y}^H\mathbf{B}^H < 0, \quad \mathbf{Q} = \mathbf{Q}^H > 0$$

$$\mathbf{I} < \mathbf{Q} < \gamma\mathbf{I},$$

$$\begin{pmatrix} \mathbf{Q} & \mathbf{Y}^H \\ \mathbf{Y} & \mu^2\mathbf{I} \end{pmatrix} > 0,$$

(10)

where the last, additional inequality ensures a limit in the control effort in the form $\max_{t \geq 0} \|\mathbf{u}\|^2 < \mu^2$. The problem (10) has to be solved for \mathbf{Q} , \mathbf{Y} and γ ; controller gains are obtained from $\mathbf{K} = \mathbf{Y}\mathbf{Q}^{-1}$. This problem is again a LMI generalized eigenvalue problem, that can be solved using standard methods²⁷.

V. RESULTS AND DISCUSSION

LMI controllers are designed wavenumber-wise, using the model of the system (5) and the design equations (10). In particular, we consider each actuation component (u , v or w on both walls) independently; a limit on the control effort $\mu = 10$, kept constant in wavenumber space, is used in the design of all controllers. In the design procedure, the linear equations pertaining to each wavenumber pair are discretized using $N = 100$ Chebyshev polynomials, and modal truncation at $N_t = 54$ (the maximum affordable size of the computational problem) is performed prior to the actual solution of the generalized eigenvalue problem (10). In addition to removing poorly resolved dynamics, modal truncation proved to be necessary due to the exacting memory requirements of the existing LMI solvers (scaling as $\approx N_t^6$); in performing modal truncation, it was thoroughly verified that the reduced order model preserves the linear transient energy growth of the unactuated system.

A. Linear analysis

The performance of LMI controllers is evaluated first in the linear setting at $Re = 2000$; in particular, perturbations at two representative wavenumber pairs are considered, namely, an oblique wave ($\alpha = 1, \beta = 1$) and a streamwise vortex ($\alpha = 0, \beta = 2$). In the results reported here, the effectiveness of different actuation components is also addressed.

The analysis reported in sec. III shows that the closed-loop system will have a non-normal behavior; it is therefore natural to contrast the maximum closed-loop transient growth G with the open-loop one, in order to verify that a consistent reduction in G is obtained via the minimization in (10). Results, obtained for the same trun-

	Oblique waves		Streamwise vortices	
	Open-loop	Closed-loop	Open-loop	Closed-loop
u - actuation	67.62	33.04	785.93	635.83
v - actuation	66.81	11.84	33126.72	129.23
w - actuation	67.13	32.70	163123.13	85.90

TABLE I: Maximum transient energy growth G for the open-loop and closed-loop cases, for the oblique wave case ($\alpha = 1, \beta = 1$) and the streamwise vortex case ($\alpha = 0, \beta = 2$), using different actuation components on both walls. $Re = 2000$.

cated system used in the design and for the two wavenumber pairs considered, are reported in table I. It is shown that, in both the oblique wave case and the streamwise vortex case, solution of (10) leads to a closed-loop system experiencing a reduced maximum transient energy growth. In particular, for the oblique wave case, v is the most effective actuation component, whereas actuating with w is most effective in the streamwise vortex case. The performance of the present controllers is further compared against full-state controllers designed with the LQR approach²³, considered in a similar transition problem by Hogberg et al.⁸. The aim of the LQR control is the minimization of the time integral of the perturbation energy, while keeping the time integral of the control effort as low as possible; in fact, the control objective is given in terms of the closed-loop minimization of a functional in the form

$$J = \int_0^{+\infty} \bar{\mathbf{x}}^H \mathbf{Q} \bar{\mathbf{x}} + \rho \mathbf{u}^H \mathbf{u} dt.$$

This is substantially different from the control objective of the present LMI formulation (10), which considers bounds on the disturbance energy and control expenditure; therefore – at a fixed control expenditure – LMI controllers can be used to estimate a possible best performance (in terms of peaking suppression) of other control strategies. In order to present a fair comparison between the LQR and the LMI formulation, we iteratively design and test a LQR controller keeping \mathbf{Q} fixed (the same used in LMI design) and ρ as a free parameter, and we evaluate the integral of the control energy $\int_0^\infty \mathbf{u}^H \mathbf{u} dt$ in closed loop until it matches the value computed for the LMI controller. The closed-loop systems, controlled via both LQR and LMI gains, are tested against the respective optimal perturbations, using v -actuation for the oblique wave case and w -actuation for the streamwise vortex case (the best performance cases reported in table I); further, for the streamwise vortex we consider the antisymmetric (with respect to the $y = 0$ plane) optimal perturbation. The time evolution of the perturbation energy is displayed in fig. 3 and 4. Results show that, at a given control expenditure, the worst-case initial condition for the LMI-controlled system experiences a lower amplification than the corresponding perturbation for the LQR-controlled system; the peak for the LMI-controlled

system occurs at later times for the streamwise vortex case. Despite the mild reduction in maximum amplification, the results shown here suggest that a control design technique directly targeting the growth mechanism is able to better exploit the degrees of freedom in the controller to achieve a minimal transient peaking of the energy.

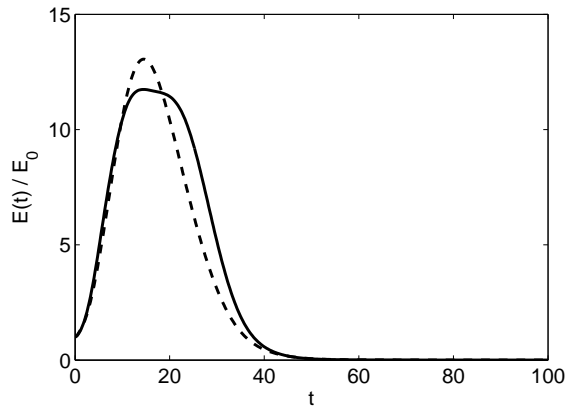


FIG. 3: Time evolution of the perturbation energy for the closed-loop system controlled using LMI gains (—) and LQR gains (---), actuation using v . The initial condition for the two systems is the respective closed-loop optimal perturbation, and the LQR gains are iteratively designed so that the energy expense over the simulated time horizon for the two closed-loop systems is the same. Results for $(\alpha = 1, \beta = 1)$ at $Re = 2000$.

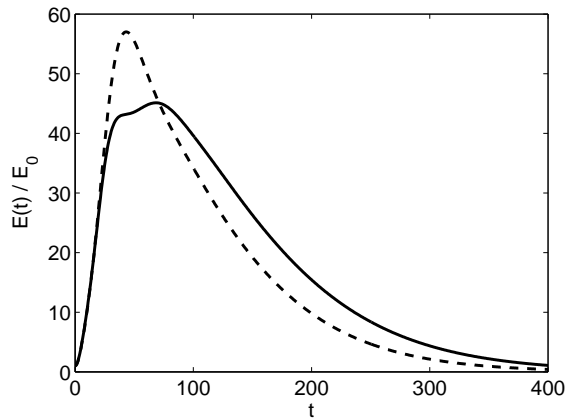


FIG. 4: Time evolution of the perturbation energy for the closed-loop system controlled using LMI gains (—) and LQR gains (---), actuation using w . The initial condition for the two systems is the respective closed-loop antisymmetric (with respect to the $y = 0$ plane) optimal perturbation, and the LQR gains are iteratively designed so that the energy expense over the simulated time horizon for the two closed-loop systems is the same. Results for $(\alpha = 0, \beta = 2)$ at $Re = 2000$.

The performance of LMI controllers is also evaluated

against optimal initial conditions for the unactuated flow, and results are reported in fig. 5 and 6. Since the closed-loop system has additional state equations associated with the dynamics of wall velocity components used as actuators, these values are set to zero, assuming that at initial time the open-loop flow satisfies the no-slip and no-transpiration condition at the walls. In particular, for the oblique wave case, it is shown that actuating with v reduces the maximum amplification of the optimal disturbance by a factor ≈ 8.2 , whereas a less effective reduction (by a factor ≈ 2.5) is obtained using u or w . Further, the growth curves in these latter cases are very close to each other, as the effect of actuators on the oblique wave is symmetric. In the antisymmetric streamwise vortex case, the most effective components are v and w (reduction by a factor ≈ 6.3 and ≈ 9.9 , respectively), whereas u has a quite poor performance (amplification reduced by a factor ≈ 1.2). The differences in performance between u and w may be interpreted with a geometric argument, as for a streamwise-invariant perturbation the u component acts in a weakly controllable direction. It is also noteworthy that, in all these cases, the control action reduces the time interval after which the initial disturbance gets to its maximum amplification.

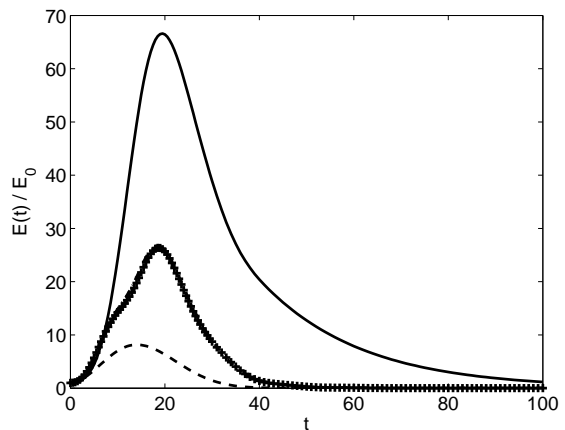


FIG. 5: Linear dynamics of the perturbation energy for the unactuated case (—), and closed-loop case actuating with u (···), v (---), w (-·-). Results for $(\alpha = 1, \beta = 1)$ at $Re = 2000$; in all cases, the initial condition is the optimal disturbance for the unactuated flow.

It is finally worth emphasizing that, when the closed-loop system experiences initial conditions in the form of optimal perturbations for the unactuated flow, the LMI and LQR performance is practically equivalent, for a given global control effort. Considering the best performing LMI controllers (v and w actuation, respectively), results are given in fig. 7 and 8, for the oblique wave and streamwise vortex. For the optimal oblique wave (fig.7), the linear evolution of the perturbation energy using LQR control matches almost perfectly that obtained with the LMI controller. In the case of antisymmetric

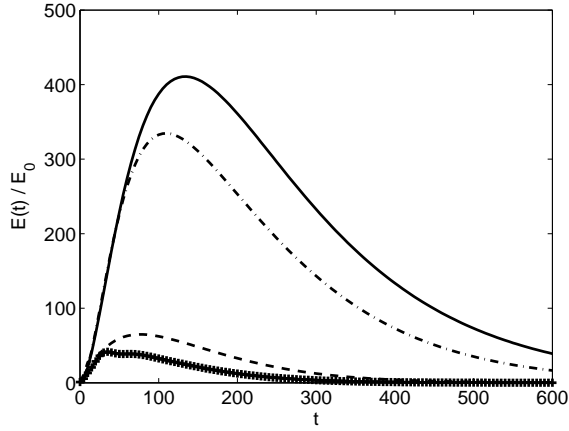


FIG. 6: Linear dynamics of the perturbation energy for the unactuated case (—), and closed-loop case actuating with u (— ·), v (— —), w (— +). Results for $(\alpha = 0, \beta = 2)$ at $Re = 2000$; in all cases, the initial condition is the antisymmetric optimal disturbance for the unactuated flow.

streamwise vortex, we obtain a slightly larger maximum amplification for the LQR, that is however followed by a faster transient to zero if compared to the LMI case. The results reported in fig. 7 and 8 are substantially independent on further decrease of the value of ρ : no significant changes in the time evolution of the perturbation energy are obtained, but at a far larger expense. This indicates that these results are close to the limit of small control weight.

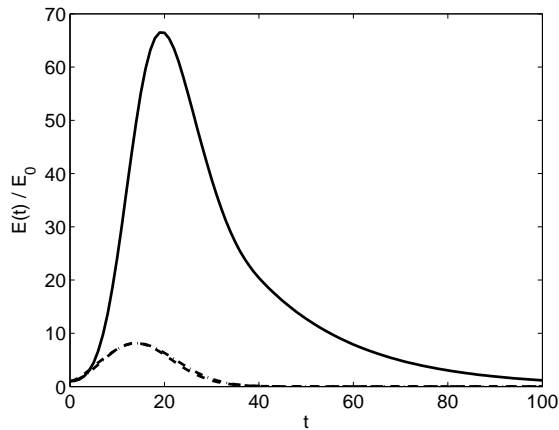


FIG. 7: Comparison of the linear evolution of the perturbation energy in unactuated case (—), closed-loop using LMI controller (— ·), and closed-loop using LQR controller (— —). Results for $(\alpha = 1, \beta = 1)$ at $Re = 2000$ ($\rho = 0.5$), actuation with v , optimal perturbation for the unactuated flow used as initial condition.

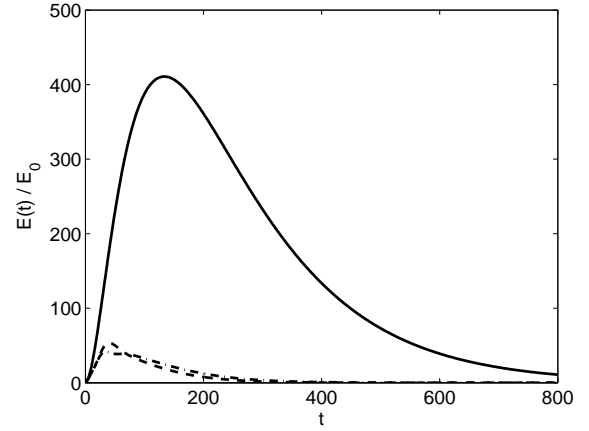


FIG. 8: Comparison of the linear evolution of the perturbation energy in unactuated case (—), closed-loop using LMI controller (— ·), and closed-loop using LQR controller (— —). Results for $(\alpha = 0, \beta = 2)$ at $Re = 2000$ ($\rho = 8.0$), actuation with w , antisymmetric optimal perturbation for the unactuated flow used as initial condition.

B. Closed-loop transition thresholds

After these numerical experiments in the linear setting, the performance of LMI-based controllers in terms of transition delay capabilities has been verified using Direct Numerical Simulations (DNS) of transitional Poiseuille flow at $Re = 2000$, using an existing computer code and computing system²⁸. Controllers are tested against initial conditions in the form of:

- a pair of oblique waves ($\alpha_0 = 1, \beta_0 = \pm 1$), in a box of size $2\pi \times 2 \times 2\pi$;
- antisymmetric streamwise vortices ($\alpha_0 = 0, \beta_0 = 2$), in a box of size $2\pi \times 2 \times \pi$.

These initial conditions are obtained by computing the optimal perturbations for the unactuated flow at the corresponding wavenumber pairs, and specifically for the streamwise vortices the optimal initial condition having antisymmetric (with respect to the centerplane $y = 0$) distribution of wall-normal velocity is considered, as it provides the optimal transition time in the nonlinear case²⁹. Random noise, in the form of a random combination of the first 30 Stokes modes – ordered by decreasing real part of the corresponding eigenvalues – is added on the wavenumber array $(0, \pm 1, \pm 2)\alpha_0$ and $(0, \pm 1, \pm 2)\beta_0$, and the noise energy is chosen as 1% of the total perturbation energy. The resulting optimal perturbations are identical to those reported in previous works^{8,29}.

In order to reduce the computational problem of control design to an affordable size, LMI controllers are designed on the same array of wavenumber pairs where random noise is introduced. Furthermore, the control effort tuning parameter is set at $\mu = 10$, a value which

is derived from preliminary tests and previous work on the control of the linearized dynamics of streamwise vortices²². The value of the parameter μ has been kept constant in wavenumber space; however, it should be emphasized that this parameter could be a function of the wavenumber pair – thus providing room for optimization of the control performance.

The performance of LMI controllers is quantified by evaluating the closed-loop transition threshold²⁹ of a given initial condition, for all the wall actuation components. The mixed spatial discretization (fourth-order, compact finite differences in y direction and Fourier expansion in x and z directions) employs 64 grid points in y and 16×64 modes in x and z . Time integration is performed via the usual semi-implicit approach, where non-linear terms are advanced explicitly using a low-storage Runge-Kutta algorithm whereas linear diffusion terms are advanced implicitly via a Crank-Nicholson scheme. Each simulation was run over a time window of 2000 nondimensional time units, that proved sufficiently long to ensure that a laminar or a turbulent state was reached after the initial transient growth of the perturbation energy. In order to obtain the thresholds reported in table II, a bisection algorithm was employed; this procedure requires a large number of simulations, corresponding to approximately 3 months of CPU time.

The open-loop transition thresholds reported in table II agree with previous findings²⁹. Results summarized in the table indicate that the LMI controller is able to increase the transitional energy of the initial conditions considered. In particular, a synthetic performance measure is indicated in the table as improvement factor (I.F.), corresponding to the ratio between the threshold energy computed in the controlled case over that corresponding to the unactuated flow. In general, for both the oblique waves and the streamwise vortices, actuation with the wall-normal velocity v outperforms actuation with the other components. This behavior is expected, as forcing with wall-parallel components affects the flow by means of viscous diffusion only, whereas forcing with v introduces an additional non-zero momentum flux at the boundary. The improvement factors associated with the oblique wave case are higher than those pertaining to the streamwise vortex case, when using u and v actuation. For the v -component case, this is coherent with previous works⁸, and can be interpreted physically by the argument that targeting oblique waves mitigates the subsequent development of streamwise vortices, therefore reducing the strength of the associated streak instability. The u component provides the overall worst performance in the streamwise vortex case, a result that can be interpreted as a consequence of the particular geometrical configuration. In fact, with respect to a streamwise-invariant spatial structure, u actuation works in an approximately null direction, whereas actuation with w is better-suited, as shown by its improvement factor. A similar geometrical interpretation can be given for the almost equal improvement factors obtained with u and w , when an pair

	Oblique waves		Streamwise vortices	
	Thres.	I.F.	Thres.	I.F.
Open-loop	$2.39 \cdot 10^{-6}$		$6.47 \cdot 10^{-6}$	
u - actuation	$9.89 \cdot 10^{-6}$	≈ 4.14	$8.57 \cdot 10^{-6}$	≈ 1.32
v - actuation	$3.04 \cdot 10^{-5}$	≈ 12.72	$4.86 \cdot 10^{-5}$	≈ 7.51
w - actuation	$9.77 \cdot 10^{-6}$	≈ 4.09	$3.86 \cdot 10^{-5}$	≈ 5.97

TABLE II: Open-loop and closed-loop transition thresholds, as measured by DNS. The values of transitional energy are given with an uncertainty of $\pm 3\%$. The column labelled I.F. indicates the improvement factor in the closed loop with respect to the unactuated case with an initial condition having the same spatial structure.

of oblique waves is given as initial condition.

Results reported in table II for the thresholds obtained using v actuation are in qualitative agreement with previous work using the LQR controllers⁸; however, in quantitative terms the LQR approach outperforms the present LMI approach. In particular, the improvement factors reported with LQR for oblique waves and streamwise vortices at $Re = 2000$ are $I.F. = 102$ and $I.F. = 10$, respectively⁸; therefore, LQR controllers seem to perform substantially better than LMI controllers in presence of oblique waves as initial conditions. It should be emphasized, however, that such comparison is not entirely appropriate. In fact, even if the same energy norm is used to quantify the magnitude of velocity disturbances, control laws are designed with different parameters constraining the control effort. As a matter of fact, the linear results reported in fig. 5 and 6 show that the LMI controller performs similarly to the LQR controller for a value of the LQR control weight $\rho = 0.5$ and $\rho = 8.0$, respectively. These values are different from the value of $\rho = 0.01$, used uniformly in wavenumber space in Högberg et al.⁸. A fair comparison between the two approaches is not possible in this case; therefore, it is impossible to draw a conclusive statement about the effectiveness of feedback minimization of transient growth versus feedback minimization of the disturbance energy in transition delay.

As the ultimate goal of LMI controllers is that of preventing transition to turbulence, it can be important to quantify the energy efficiency of these controllers in the nonlinear case. For instance, given a transitional initial condition, it is possible to compare the energy expenditure of the controller to prevent transition with the additional energy to be introduced into the unactuated flow to compensate for the increase in friction, over the same time window (i.e. the time necessary for the transient in the controlled flow to die out). Referring to the best performing cases in table II, we consider actuation with wall-normal velocity v and, in the two cases, initial conditions having energy $\approx 3\%$ below the corresponding closed-loop threshold. Using the present nondimensionalization, a conservative estimate of the energy required for the control action in the time interval $[0, T]$ can be

given by¹¹:

$$E_c = \frac{1}{V} \int_0^T \int_{A_{u,l}} (|\frac{v^3}{2}| + |pv|) dA dt,$$

where p is the fluctuating wall pressure and $A_{u,l}$ the upper and lower blowing/suction surfaces, whereas the additional energy required to drive the unactuated flow against the increased viscous drag on the same time interval is given by:

$$E_\nu = \frac{1}{V} \int_0^T \int_{A_{u,l}} \frac{1}{Re} \left(\frac{\partial U}{\partial y} - \frac{\partial U_{lam}}{\partial y} \right) dA dt.$$

The ratio E_c/E_ν reads about $1.39 \cdot 10^{-3}$ and $1.68 \cdot 10^{-3}$, for the oblique waves and streamwise vortex case, respectively. Furthermore, linear tests using v actuation have shown that E_c can be of the same order of magnitude of the actual reduction in maximum transient energy growth. Hence, these results indicate that, even if the energy expenditure due to the control action is comparable to that experienced in the linear amplification of the optimal disturbance, it is nevertheless negligible if compared to the potential energy saving due to transition prevention.

VI. CONCLUSIONS

The present work has considered the design of full-state feedback controllers specifically targeting the transient energy growth mechanism in laminar channel flow. It

has been shown that full transpiration at both walls and full-state knowledge are not sufficient to ensure a monotonically stable closed-loop system via a linear feedback law. Further, an advanced control design technique – based on a LMI formulation – has been employed to design feedback controllers that have been tested in both the linearized setting and in nonlinear, transitional flows.

Linear tests indicated that the LMI strategy allows to obtain a consistent reduction of the maximum open-loop transient growth. At a given global control expenditure over a time window sufficiently long for the perturbations to decay to zero, the LMI-controlled closed-loop system experiences a lower transient energy amplification than a LQR-controlled closed-loop flow. However, in presence of an optimal perturbation for the unactuated flow, the performance of the two control strategies is practically equivalent. Results obtained in the linear setting further indicate that, in the case of perturbations in the form of oblique waves and streamwise vortices, the most effective actuation components are v and w , respectively.

In the nonlinear case, it has been found that these controllers are capable of increasing the threshold energy for transition when initial conditions are given to the flow in the form of oblique waves or streamwise vortices; the effectiveness of different actuation components has been addressed, indicating that wall blowing/suction is most effective in providing a higher closed-loop threshold energy. Additionally, in transitional conditions, LMI controllers prove to be energy-effective, as the energy required by the control action is negligible when compared to the energy saving due to avoiding transition.

-
- ¹ K.M. Butler and B.F. Farrell. Three-dimensional optimal perturbations in viscous shear flow. *Phys. Fluids*, 4(8):1637–1650, 1992.
 - ² S.C. Reddy and D.S. Henningson. Energy growth in viscous channel flows. *J. Fluid Mech.*, 252:209–238, 1993.
 - ³ P.J. Schmid and D.S. Henningson. Optimal energy density growth in Hagen-Poiseuille flow. *J. Fluid Mech.*, 277:197–255, 1994.
 - ⁴ P. J. Schmid and D. S. Henningson. *Stability and transition in shear flows*. Springer, 2000.
 - ⁵ P. J. Schmid. Nonmodal stability theory. *Ann. Rev. Fluid Mech.*, 39:129–162, 2007.
 - ⁶ S. S. Joshi, J. L. Speyer, and J. Kim. A systems theory approach to the feedback stabilization of infinitesimal and finite-amplitude disturbances in plane Poiseuille flow. *J. Fluid Mech.*, 332(157), 1997.
 - ⁷ T.R. Bewley and S. Liu. Optimal and robust control and estimation of linear paths to transition. *J. Fluid Mech.*, 365:305–349, Jun 1998.
 - ⁸ M. Högberg, T.R. Bewley, and D.S. Henningson. Linear feedback control and estimation of transition in plane channel flow. *J. Fluid Mech.*, 481:149–175, Apr 2003.
 - ⁹ J. Kim and J. Lim. A linear process in wall-bounded turbulent shear flows. *Phys. Fluids*, 12(8):1885–1888, 2000.
 - ¹⁰ K. Lee, L. Cortelezzi, J. Kim, and J. L. Speyer. Application of reduced-order controller to turbulent flows for drag reduction. *Phys. Fluids*, 13(5):1321–1330, 2001.
 - ¹¹ T. R. Bewley, P. Moin, and R. Temam. DNS-based predictive control of turbulence: an optimal benchmark for feedback algorithms. *J. Fluid Mech.*, 447:179–225, 2001.
 - ¹² J. Kim. Control of turbulent boundary layers. *Phys. Fluids*, 15(5):1093–1105, 2003.
 - ¹³ T. R. Bewley. Flow control: new challenges for a new Renaissance. *Prog. Aero. Sci.*, 37:21–58, 2001.
 - ¹⁴ P. Corbett and A. Bottaro. Optimal control of nonmodal disturbances in boundary layers. *Theor. Comp. Fluid Dyn.*, 15:65–81, 2001.
 - ¹⁵ S. Zuccher, P. Luchini, and A. Bottaro. Algebraic growth in a Blasius boundary layer: optimal and robust control by mean suction in the nonlinear regime. *J. Fluid Mech.*, 513:135–160, 2004.
 - ¹⁶ H.J. Sussmann and P.V. Kokotovic. The peaking phenomenon and the global stabilization of nonlinear systems. *IEEE Trans. Autom. Control*, 36(4):424–440, 1991.
 - ¹⁷ E. Plischke and F. Wirth. Stabilization of linear systems with prescribed transient bounds. In *Proc. 16th Int. Symp. Math. Theory Net. Syst.*, Leuven, Belgium, 2004.
 - ¹⁸ E. Plischke. *Transient effects of linear dynamical systems*.

- PhD thesis, Universitat Bremen, Germany, 2005.
- ¹⁹ J.F. Whidborne and J. McKernan. On the minimization of maximum transient energy growth. *IEEE Trans. Autom. Control*, 52(9):1762–1767, 2007.
 - ²⁰ J.F. Whidborne, J. McKernan, and G. Papadakis. Minimising transient energy growth in plane Poiseuille flow. *Proceedings Inst. Mech. Eng., Part I, J. Syst. Control Eng.*, 222(15):323–331, 2008.
 - ²¹ F. Martinelli, M. Quadrio, J. McKernan, and J. F. Whidborne. Feedback control of transient energy growth in subcritical plane Poiseuille flow. In D. S. Henningson and P. Schlatter, editors, *Seventh IUTAM Symposium on Laminar-Turbulent Transition*, volume 18, 2009.
 - ²² J. McKernan. *Control of Plane Poiseuille Flow: A Theoretical and Computational Investigation*. PhD thesis, Department of Aerospace Sciences, School of Engineering, Cranfield University, 2006.
 - ²³ S. Skogestad and I. Postlethwaite. *Multivariable Feedback Control*. Wiley, Chichester, England, 1996.
 - ²⁴ W. Lohmiller and J. J. Slotine. On contraction analysis for nonlinear systems. *Automatica*, 34, 1998.
 - ²⁵ M. Högberg, T. R. Bewley, and D. S. Henningson. Relaminarization of $Re_\tau=100$ turbulence using gain scheduling and linear state-feedback control. *Phys. Fluids*, 15(11):3572–3575, 2003.
 - ²⁶ S. Boyd, L. El Ghaoui, E. Feron, and V. Balakrishnan. *Linear matrix inequalities in system and control theory*. SIAM, Philadelphia, 1994.
 - ²⁷ Y. Nesterov and A. Nemirovskii. *Interior-point polynomial algorithms in convex programming*. SIAM, 1994.
 - ²⁸ P. Luchini and M. Quadrio. A low-cost parallel implementation of direct numerical simulation of wall turbulence. *J. Comp. Phys.*, 211(2):551–571, 2006.
 - ²⁹ S. C. Reddy, P. J. Schmid, J. S. Baggett, and D. S. Henningson. On stability of streamwise streaks and transition thresholds in plane channel flows. *J. Fluid Mech.*, 365:269–303, 1998.